Enhanced Efficiency of Graphene-silicon Schottky Junction Solar Cell through Pyramid Arrays Texturation

Cheng Li
Kunming University of Science and Technology
Yichen Ma
Yunnan University
Xiyao Zhang
KUST
Xiuhua Chen
Yunnan University
Fengshuo Xi
KUST
Shaoyuan Li (lsy415808550@163.com)
KUST https://orcid.org/0000-0002-8124-8408
Ma Wenhui
KUST
Yuanchih Chang
University of new south wales

Research Article

Keywords: Gr/Si solar cells, TMAH, Surface texturing, Silicon pyramid array

Posted Date: September 16th, 2021

DOI: https://doi.org/10.21203/rs.3.rs-872635/v1

Version of Record: A version of this preprint was published at Silicon on January 16th, 2022. See the published version at https://doi.org/10.1007/s12633-021-01579-2.

Abstract

Graphene/silicon (Gr/Si) Schottky junction solar cells have attracted extensive research interest due to their simple structure and potential low-cost. Surface texturing is an important part of high-efficiency solar cells. In this paper, the effects of TMAH concentration, IPA concentration and etching time on the structure and anti-reflection ability of silicon pyramid array (SiPa) were systematically studied to obtain uniform and reliable pyramid array. Under the optimized conditions, a large scale SiPa with uniform size distribution was obtained and applied to Gr/Si solar cells. The results show that the TMAH etched SiPa has a better Schottky junction contact between graphene and the SiPa surface, and the SiPa can further improves the ability of collecting photogenerated carriers. Compared with Gr/Si solar cells, the power conversion efficiency (PCE) of Gr/SiPa device is 1.66 times higher than that of Gr/Si solar cells. Finally, Gr/SiPa devices with PCE of 5.67% is successfully obtained by HNO_3 doping. This work proposes a new strategy for TMAH etching SiPa to improve the performance of Gr/Si solar cells.

1 Introduction

The mission of carbon emission reduction are pushing the global energy structure toward a cleaner and more sustainable development. For this reason, photovoltaic technology and industries are getting unprecedented attention and development[1–2]. At present, crystalline silicon solar cell due to its abundant raw materials, mature preparation technology and excellent stability occupy the main commercial solar cells market[3–6]. However, the high cost and high energy consumption of p-n junction is probably contrary to the development goal of green and clean energy saving and emission reduction[7–10]. Therefore, reducing the cost of solar cell preparation, simplifying the preparation process, and developing solar cells that combine abundant silicon materials to produce simple device structures at low temperature have always been the focus of current research.

In recent years, a new type of Schottky junction solar cell developed by combining graphene with silicon has attracted extensive attention[11–13]. Gr/Si solar cells were prepared by a simple room temperature wet transfer process. In this structure, the light can directly penetrate the graphene film to the Schottky junction, and the excited pairs of electron holes in the silicon are separated by a built-in electric field, generating a photocurrent. Gr/Si solar cells avoid the complex process of p-n/p-i-n junction formation in traditional silicon solar cells, and also facilitate light absorption and carrier separation and transport[14–16]. Therefore, Gr/Si solar cells provide a new idea for the preparation of solar cells with simple structure at low temperature.

The light reflection on the surface of solar cells is one of the key factors limiting their performance, because the high reflectivity of silicon wafers affects the efficient generation of electron-hole pairs in the cells[17–19]. It is necessary to reduce the reflectivity of silicon wafers to improve the conversion efficiency of solar cells. Silicon nanostructures have great attraction in the application of solar cells because of their high efficient anti-reflection (AR) effect. Fan et al.[20] prepared silicon nanowires on the surface of silicon wafer by Ag-assisted chemical etching to improved the light absorption of silicon

substrate, and the efficiency of Gr/Si solar cell reached 2.86% through chloride doping. The photolithography and inductive couple plasma (ICP) etching were employed to fabricate the silicon pillar array and the efficiency of the cell increased from 1.96–3.55% under HNO_3 doping[21]. Dong Hee Shin et al.[22] successfully prepared graphene/porous silicon solar cells with an efficiency of 2.32%, and under the doping of silver nanowires(AgNWs), the power conversion efficiency (PCE) was improved to 4.03%. Tetramethyl ammonium hydroxide (TMAH) is widely used in microelec-tromechanical systems (MEMS) and nanoelectromechanical systems (NEMS) based sensors and actuators because of its non-toxic, easy removal, no metal ion contamination and good anisotropic corrosion characteristics[23–24]. Currently, many studies were reported about smooth surfaces for MEMS and NEMS obtained by TMAH etching, but only few results were reported about silicon surface texture to improve the light capture in solar cells.

In this study, the effects of TMAH concentration, IPA concentration and etching time on the morphology and reflection spectra of silicon wafers were systematically studied. Then, the graphene/silicon pyramid (Gr/SiPa) Schottky junction solar cells were prepared by using the large-scale uniform silicon pyramid array obtained under the optimal parameters, and the efficiency reached 5.67% under HNO_3 doping. In this paper, we propose a new strategy to introduce pyramid arrays prepared by TMAH etching to improve the performances of Gr/Si solar cells.

2 Experimental

2.1 Preparation and transfer of graphene films

The few-layer graphene film was prepared on the Cu foils by plasma-enhanced chemical vapor deposition (PECVD)[25–27]. The resulting graphene films were transferred to n-type silicon wafers by cyclododecane supported etching at room temperature. First, a mixture of cyclododecane and cyclohexane with a mass ratio of 1:1 was spin-coated on the graphene films surface as supporting layer, and the copper substrate was etched away by etchant of $FeCl_3$:HCl:$H_2$0 = 20 g:15 ml:185 ml. After that, the graphene was repeatedly rinsed with deionized water to completely remove the residue.

2.2 Preparation of silicon pyramid arrays (Sipa) texturation

N-Type (100) Si wafers (resistivity of 1–10 $\Omega \cdot cm^{-1}$) with 100 nm thick SiO_2 oxidation layer were used as substrates in our study. Si wafers were firstly cleaned in acetone, ethanol, and deionized water for 15 min by ultrasound. An opening window of 3×3 mm^2 defined on the SiO_2/Si substrate by an adhesive tape as the effective work area of the graphene/silicon solar cell. The SiO_2 insulative layer within the window was removed by the diluted 5% (v/v) HF solution to expose the Si surface, followed by rinsing in deionized (DI) water for 3 ~ 5 min. Subsequently, these Si wafers were put in the TMAH-IPA alkaline etching solution to prepare Sipa texturation, and the detailed experimental conditions were shown in the Table 1, Tables 2 and 3. Then was rinsed using deionized water. Finally, the SiO_2/Si substrate was dried by nitrogen gas stream and the adhesive tapes on the SiO_2/Si substrate were peeled off.

2.3 Fabrication of photovoltaic devices

The schematic of fabrication flow of Gr/SiPa Schottky junction solar cells were showed in Fig. 1. The SiPa substrates were formed through the process of TMAH-IPA alkaline etching process (as described in Sect. 2.2). Then, the graphene film was transferred onto the SiPa substrate by a cyclododecane-based transfer method at room temperature, followed cyclododecane on the graphene film was then removed by annealing at 400 ℃ for 20min, and the graphene was fully contacted with silicon to form a Schottky junction. Finally, Silver paste and Indium-gallium (In-Ga) eutectic alloy were used as front electrode and back electrode of photovoltaic devices respectively.

2.4 Characterizations of materials and devices

The morphology of texturing samples surfaces was analyzed by scanning electron microscopy (SEM, Nova NanoSEM 450). The reflectance measurement was carried out on a spectrophotometer (UV- 2550). The characteristics of photovoltaic devices were collected by a Keithley 2420 source meter and a AAA solar simulator under AM 1.5 G with an irradiation intensity of 100 mW/cm^2.

3 Results And Discussion

3.1 Effect of TMAH concentration on Sipa texturation

In order to investigate the effect of TMAH concentration on the pyramid structure of silicon surface, four kinds of samples were prepared at the mass concentration of TMAH of 1%, 2%, 3% and 4% respectively. The IPA concentration and etch time were fixed at 10% and 30 min, respectively. The silicon wafers were placed in etch solution of 80 ℃ for constant temperature reaction, and the samples were characterized by SEM. The detailed experimental conditions were shown in the Table 1.

Figure 2 shows that the SEM diagram of SiPa under different TMAH concentrations. It can be seen that with the increase of TMAH concentration, the size of silicon pyramid has obvious changes. When TMAH concentration is 1%, there are still many parts on the silicon surface that are not etched to form silicon pyramid, and the etched silicon pyramid has different sizes. When the TMAH concentration increases to 2%, the pyramid structure on the silicon surface covers the whole silicon chip, and the size of the pyramid is evenly distributed. When the TMAH concentration increases to 3%, a small number of relatively large silicon pyramid structures will appear, which affects the overall uniformity of the silicon pyramid array. When the concentration of TMAH is further increased to 4%, it can be found that some small silicon pyramids are embedded in the large silicon pyramids.

Figure 3 shows the reflectance spectra of the samples at different TMAH concentrations in the wavelength range of 300~1200 nm. It can be found that the reflectance of the sample decreases with the increase of TMAH concentration. When the TMAH concentration increases to 2%, the reflectance is the lowest, and the average reflectance can reach 12.07%. After increasing the TMAH concentration, the

sample reflectivity decreases. This phenomenon can be explained by the etching reaction mechanism of TMAH solution on silicon wafers.

The formula of etching reaction of TMAH solution on silicon wafer is as follows[28]:

(1) TMAH is decomposed into OH^- and TMA^+($(CH_3)_4N^+$) ions in solution:

$$(CH_3)_4NOH \rightarrow (CH_3)_4N^+ + OH^- \quad (1)$$

(2) Redox reaction takes place in the solution, and the silicon wafer is etched by anisotropy, forming the pyramid structure of silicon:

$$Si + 2OH^- + H_2O \rightarrow SiO_3^{2-} + 2H_2\uparrow \quad (2)$$

(3) The entire etching reaction of silicon wafer in TMAH solution is:

$$Si + 2(CH_3)_4NOH + H_2O \rightarrow 2(CH_3)_4N^+ + SiO_3^{2-} + 2H_2\uparrow \quad (3)$$

According to equation (1) of reaction, when the concentration of TMAH increases, a large amount of OH^- will be generated, which accelerates the etching rate. When the concentration is higher, TMAH isotropic etching mainly controls the whole reaction process[29]. According to equation (2) of the reaction, with the progress of the reaction, the concentration of OH^- gradually decreases, and the generated $(CH_3)_4N^+$ and SiO_3^{2-} will be adsorbed on the surface of the silicon chip, thus inhibiting the reaction between OH^- and the silicon chip and slowing down the etching rate. In this process, there will be a chemical reaction mechanism of TMAH to enhance the anisotropic etching of silicon wafer and weaken the isotropic etching[30-32]. Therefore, in the whole reaction mechanism, reasonable control of TMAH concentration can obtain the silicon pyramid structure array with uniform size and full of silicon wafers, and the reflectivity is the lowest at this time.

3.2 Effect of IPA concentration on Sipa texturation

In order to explore how the IPA concentration affected the pyramid structures on the silicon surface, four samples were prepared under different IPA concentration of 0%, 5%, 10% and 15%. The TMAH concentration and etch time were respectively fixed as 2% and 30 min (as shown in Table 2). The silicon wafers were placed in etch solution of 80 ℃ for constant temperature reaction. After etching, the samples were directly characterized via SEM.

As a common surfactant, IPA does not directly participate in the etching process of silicon wafers[33]. However, when IPA is contained in TMAH etching solution, it can prevent the H_2 bubbles generated by the reaction from adhering to the surface of the silicon wafer, and reduce the surface tension of the silicon wafer, increase the surface wettability, weaken the etching strength of the etching solution, increase the

anisotropy of the etching, which is conducive to the nucleation and growth of the silicon pyramid. Figure 4 shows the SEM of SiPa under different IPA concentrations, With the addition of IPA, it can be seen that the uniformity of SiPa has been significantly improved. As shown in figure 4(a), when there is no IPA in the etching solution, the size of silicon pyramids varies greatly, and some silicon wafer surfaces do not have pyramids. This is because the etching rate of the reaction is fast at this time, and a large amount of H_2 is generated to attach to the silicon surface with bubbles of different sizes. Therefore, the region etching reaction rates were different and the size of silicon pyramids were greatly different. With the increase of IPA concentration, the size of the silicon pyramid on the surface becomes consistent, covering the whole silicon wafers were showed in figure 4(b)-(c). This is because with the increase of IPA concentration, the wettability of the solution decreases, the H_2 bubbles attached to the silicon wafer become smaller, and the etching rate decreases. However, too high concentration of IPA will obviously slow down the etching rate[34]. In a certain period of time, the reaction is not sufficient, resulting in part of the pyramid is not formed was showed figure 4(d).

The reflectivity of silicon etchings at different IPA concentrations was shown in figure 5. It can be seen that without IPA, the reflectivity of silicon wafer is the highest, which is caused by the different sizes of silicon pyramids. There are few pyramids with effective reduction on the surface of silicon wafer, which is not conducive to light absorption. When IPA concentration increases, the uniformity of pyramid increases and it covers the whole silicon chip, which can effectively reflect light multiple times, thus reducing the reflectivity. When IPA concentration is 10%, the reflectivity is the lowest. When the concentration of IPA increases to 15%, the high concentration of IPA inhibits the etching rate, resulting in the unformed positive pyramid in some areas and the increase of reflectivity.

3.3 Effect of etching time on Sipa texturation

In order to explore how the etching time affected the pyramid structures on the silicon surface, four samples were prepared under different etching time of 10 min, 20 min, 30 min and 40 min. The TMAH concentration and IPA concentration were respectively fixed as 2% and 10% (as shown in Table 3). The silicon wafers were placed in etch solution of 80 ℃ for constant temperature reaction. The samples were characterized by SEM.

Compared with SEM images of SiPa at different etching time in figure 6. It can be found that the silicon pyramids were nucleated when etched for 10 min. As the etch time increases to 20 min, the silicon pyramids were grown and formed, forming the silicon pyramid with obvious pyramidal structure and different sizes. When the etch time is increased to 30 min, the size of the silicon pyramids were becomed more uniform and completely covers the entire surface of the silicon chip. However, with the prolongation of etching time (40 min), part of the large silicon pyramids were etched away and became a small pyramid structure, with obvious difference in size, decreased uniformity and pits in some areas.

The reflectance of silicon wafer samples etched at different times was shown in figure 7. The reason for the high reflectivity of silicon wafer after etching for 10 min is that the silicon pyramids were nucleated and had not formed a complete pyramid structure. When the etching time is extended to 20 min to 30 min, the morphology and distribution of silicon pyramids were gradually becomed more uniform. The reflectivity was decreased to the lowest 12.07% when the etching time is 30 min. At this time, the SiPa has a good anti-reflection effect. When the etching time increases to 40 min, the reflectance increases to 16.85%. The main reason is that with the increase of the etching time, the original intact pyramids were etched and appeared pits, which affected the uniformity and integrity of the SiPa and caused the rise of surface reflectance.

3.4 Study on photovoltaic performance of Gr/SiPa Schottky junction solar cells

In order to study the effect of SiPa on the performance of Gr/Si solar cells, the SiPa with excellent anti-reflection performance was prepared by etching with TMAH concentration of 2% and IPA concentration of 10% for 30 min, and the Gr/planar Si solar cells were prepared at the same time. Figure 8(a) shows the *J-V* characteristic curves of Gr/planar Si solar cells and Gr/SiPa solar cells under illumination. As expected, the SiPa devices showed better photovoltaic performance compared to Gr/planar Si solar cells. The PCE of Gr/Planar Si solar cells is 1.09%, $V_{OC,}$ J_{SC} and fill factor (FF) are 0.43 V, 13.11 mA/cm^2 and 19.16%, respectively. However, the Gr/SiPa solar cells prepared on the silicon surface by the SiPa increased PCE by 1.66 times, V_{OC} is 0.45 V, J_{SC} is 23.38 mA/cm^2, and FF is 27.40%. It can be seen that V_{OC}, J_{SC} and FF of the device have improved, while J_{SC} has the most significant improvement. The enhancement of J_{SC} is mainly due to the fact that the silicon surface with the pyramid structure can absorb a large amount of incident light. The reflectivity of the SiPa is 12.07% in the entire visible and near infrared region, while the reflectivity of planar silicon is almost over 40%.

Figure 8(b) and (c) show the *J-V* characteristics and corresponding ln*J-V* curves of Gr/Planar Si and Gr/SiPa solar cells in the dark. The *J-V* characteristic curve in the dark shows that the solar cell prepared by the formation of Schottky junction has good rectification characteristics. In order to provide more insights into the effects of SiPa on Gr/Si solar cell performance, we further analyze their *J-V* characteristic curves. According to the thermal emission theory, The *J-V* characteristics of Gr/Si solar cells are mainly determined by the majority of carriers, and most of the (electron) current can be made by

$$J = J_O\left[\exp\left(\frac{qV}{nkT}\right)-1\right] \qquad (1)$$

Where n is the ideal factor, k is boltzmann constant, T is the thermodynamic absolute temperature, and q is the elementary charge. J_o is the reverse dark-saturation current density, which is expressed as a function of the Schottky barrier height:

$$J_O = A^* T^2 \exp(-\frac{\phi_b}{kT}) \qquad (2)$$

Where A^* represents the effective Richardson constant (≈112 A·cm^{-2}·K^{-2} for n-Si), represents Schottky barrier height.

Gr/planar Si and Gr/SiPa solar cells Schottky barriers height and ideal factors (*n)* can be extracted in figure8(c). It can be found that Schottky barrier heights are almost equal (see Table 4), which indicates that although the SiPa prepared by TMAH etching increases the specific surface area of the silicon surface, it does not cause relatively large defects on the silicon surface, resulting in serious carrier recombination[35-36]. The *n* of Gr/planar Si and Gr/SiPa Schottky junctions are 5.51 and 4.16, respectively. It is worth noting that the *n* of Schottky junction can measure the dominant degree of interface defects in the total recombination. The lower *n* goes, the closer it gets to 1. It indicates that the device is closer to the ideal junction and the better the cell performance[37]. The *n* of Gr/SiPa is lower than that of Gr/planar Si, which is mainly attributed to the uniform size of the SiPa prepared by TMAH etching. The contact area between graphene and the SiPa is larger than that of planar silicon, and a good Schottky junction contact is formed[38]. Meanwhile, the SiPa further improves the ability of silicon to collect photogenerated carriers. Better Schottky junction contact between Gr and Si leads to higher V_{OC}, which is closely related to *Jsc* according to its *J-V* relationship of:

$$V_{OC} = \frac{nkT}{q} In\left(\frac{J_{SC}}{J_0} + 1\right) \approx \frac{nkT}{q} In\frac{J_{SC}}{J_0} \qquad (3)$$

It can be seen that the value of V_{OC} is tied to J_{SC} in principle, and the increase of V_{OC} of Gr/SiPa solar cells is due to the enhancement of J_{SC}[39]. Figure 8(d) is d*V*/d(ln*J*)-*J* curve, and series resistance (R_s) can be deduced from the slope of the curve by linear fitting. It can be seen that when the SiPa is introduced on the silicon surface, R_s decreases from 7.5 Ω·cm^2 to 7.0 Ω·cm^2, and the shunt resistance (R_{sh}) increases from 243.7 Ω·cm^2 to 289.4 Ω·cm^2, which is conducive to the increase of FF.

Although we took a simple method to fabricate the original Gr/SiPa solar cells, there still exists a major problem of low PCE due to the relatively low electrical conductivity of graphene. To further improve device PCE, graphene was chemically doped. After HNO_3 doping, PCE of the Gr/SiPa solar cells increased from

2.90% to 5.67%, FF significantly increased from 27.40% to 52.53%, V_{OC} and J_{SC} increased from 0.45 V and 23.38 mA/cm^2 to 0.49 V and 31.07 mA/cm^2, respectively (as shown in figure 9). This is mainly attributed to the p-type doping of graphene formed by HNO_3, which effectively improves the conductivity of graphene[40]. Finally, the PCE of HNO_3/Gr/SiPa Schottky junction solar cells is 5.67%, which is higher than other Gr/Si solar cells with silicon nanowires and porous silicon structure. This work provides a new strategy for introducing SiPa prepared by TMAH etching to improve the performance of Gr/Si solar cells.

4. Conclusions

In summary, the effects of TMAH concentration, IPA concentration and etching time on the silicon pyramid structure array were systematically studied, and a large scale silicon pyramid array with uniform size distribution was successfully prepared on the surface of silicon wafer, and good anti-reflection ability was obtained. The silicon pyramid array with the lowest average reflectivity (12.07%) was successfully prepared under optimized conditions of 2% TMAH, 10% IPA and etched for 30 min. The Gr/SiPa Schottky junction solar cells were successfully prepared by introducing SiPa into Gr/Si solar cells, and the PCE was 2.66 times higher than that of planar silicon. As a result, the improvement of cell performance is mainly due to the uniform size of the SiPa prepared by TMAH etching, which makes the contact area between graphene and the SiPa larger than that of planar silicon, and forms a good Schottky junction contact. Meanwhile, the SiPa further improves the ability of silicon to collect photogenerated carriers. Chemically doped HNO_3 on graphene is an effective way to improve cell performance. Finally, the Gr/SiPa Schottky junction solar cells with efficiency of 5.67% were successfully achieved after HNO_3 treatment. In this paper, a new strategy is proposed to introduce the SiPa prepared by TMAH etching to improve the performance of Gr/Si solar cells.

Declarations

Acknowledgments

Financial support of this work from the National Natural Science Foundation of China (Grant No. 51974143, 51904134, 61764009, 51762043); National Key R&D Program of China (No. 2018YFC1901801, No. 2018YFC1901805); Major Science and Technology Projects in Yunnan Province (No. 2019ZE007, No. 202103AA080004, No. 202102AB080016); Key Project of Yunnan Province Natural Science Fund (No. 2018FA027); Yunnan Ten Thousand Talents Project (YNWR-QNBJ-2018-111) and the Program for Innovative Research Team in University of Ministry of Education of China (No. IRT_17R48).

Conflicts of interest

The authors declare that they have no known competing financial interests or personal relationships that could have appeared to influence the work reported in this paper.

Availability of data and material

The authors declare that the data and materials for this work are available.

Code availability

Not applicable.

Authors' contributions

Cheng Li: Data curation, Writing - original draft. Yichen Ma: Conceptualization. Xiyao Zhang: Software. Xiuhua Chen: Funding acquisition, Visualization, Investigation. Fengshuo Xi: Supervision, Writing -review & editing. Shaoyuan Li: Funding acquisition, Supervision, Writing -review & editing. Wenhui Ma: Funding acquisition, Supervision. Yuanchih Chang: Writing - review & editing.

Ethics approval

The authors declare that the manuscript is not currently being considered for publication in another journal.

Consent to participate

I testify on behalf of all co-authors that our article submitted to *Silicon*.

Consent for Publication

The authors agree that the manuscript should be published in *Silicon*.

References

1. Xi F, Li S, Ma W, Chen Z, Wei K, Wu J (2021) A review of hydrometallurgy techniques for the removal of impurities from metallurgical-grade silicon. Hydrometallurgy 201(9):105553
2. Luo Q, Ma H, Hou Q, Li Y, Ren J, Dai X, Yao Z, Zhou Y, Xiang L, Du H, He H, Wang N, Jiang K, Lin H, Zhang H, Guo Z (2018) All-carbon-electrode-based endurable flexible perovskite solar cells. Adv Func Mater 28(11):1706777
3. Powell DM, Winkler MT, Choi HJ, Simmons CB, Needleman DB, Buonassisi T (2012) Crystalline silicon photovoltaics: a cost analysis framework for determining technology pathways to reach baseload electricity costs. Energy Environ Sci 5(3):5874–5883

4. Taguchi M, Yano A, Tohoda S, Matsuyama K, Nakamura Y, Nishiwaki T, Fujita K, Maruyama E (2013) 24.7% record efficiency hit solar cell on thin silicon wafer. IEEE J Photovolt 4(1):96–99
5. Wang Y, Xia Z,Liu L, Xu W, Yuan Z, Zhang Y (2017) The Light-Induced Field-Effect Solar Cell Concept–Perovskite Nanoparticle Coating Introduces Polarization Enhancing Silicon Cell Efficiency. Advanced Materials 29(18):1606370.1-1606370.7
6. Liu J, Ji Y, Liu Y, Xia Z, Han Y, Li Y, Sun B (2017) Doping-Free Asymmetrical Silicon Heterocontact Achieved by Integrating Conjugated Molecules for High Efficient Solar Cell. Advanced Energy Materials 1700311:1–7
7. Battaglia C, Cuevasb A, De Wolf S (2016) High-efficiency crystalline silicon solar cells: status and perspectives. Energy Environmental Science Ees 9:1552–1576
8. Li C, He Z, Wang Q, Liu J, Li S, Chen X, Ma W, Chang Y (2021) Performance improvement of PEDOT:PSS/N-Si heterojunction solar cells by alkaline etching. Silicon (1):1–9
9. Liu J, Yao Y, Xiao S, Gu X (2018) Review of status developments of high-efficiency crystalline silicon solar cells. J Phys D: Appl Phys 51(12):123001
10. Xu D, Yu X, Gao D, Li C, Zhong M, Zhu H, Yuan S, Lin Z, Yang D (2016) Self-generation of a quasi p–n junction for high efficiency chemical-doping-free graphene/silicon solar cells using a transition metal oxide interlayer. Journal of Materials Chemistry A 4(27):10558–10565
11. Chen CC, Aykol M, Chang CC, Levi AFJ, Cronin Stephen B (2011) Graphene-silicon Schottky diodes. Nano Lett 11(5):1863–1867
12. Luongo G, Grillo A, Urban F, Giubileo F, Bartolome AD (2019) Effect of silicon doping on graphene/silicon Schottky photodiodes. Materials Today: Proceedings 20:82–86
13. Behura SK, Wang C, Wen Y, Berry V (2019) Graphene–semiconductor heterojunction sheds light on emerging photovoltaics. Nat Photonics 13(5):312–318
14. Geng C, Shang Y, Qiu JJ, Wang Q, Chen X, Li S, Ma W, Fan H, Omer AAA, Chen R (2020) Carbon quantum dots interfacial modified graphene/silicon Schottky barrier solar cell. J Alloy Compd 835:155268
15. Zhang X, Xie C, Jie J, Zhang X, Wu Y, Zhang W (2013) High-efficiency graphene/Si nanoarray Schottky junction solar cells via surface modification and graphene doping. Journal of Materials Chemistry A 1(22):6593–6601
16. Kong X, Zhang L, Liu B, Gao H, Zhang Y, Yang H, Song X (2019) Graphene/Si Schottky solar cells: a review of recent advances and prospects. RSC Advances 9(2):863–877
17. Li S, Ma W, Chen X, Xie K, Li Y, He X, Yang X, Lei Y (2016) Structure and antireflection properties of SiNWs arrays form mc-Si wafer through Ag-catalyzed chemical etching. Appl Surf Sci 369(30):232–240
18. Ozdemir B, Kulakci M, Turan R, Unalan HE (2011) Effect of electroless etching parameters on the growth and reflection properties of silicon nanowires. Nanotechnology 22(15):155606

19. Geng X, Li M, Zhao L, Bohn PW (2011) Metal-assisted chemical etching using tollen's reagent to deposit silver nanoparticle catalysts for fabrication of quasi-ordered silicon micro/nanostructures. J Electron Mater 40(12):2480–2485
20. Fan G, Zhu H, Wang K, Wei J, Li X, Shu Q, Guo N, Wu D (2011) Graphene/silicon nanowire Schottky junction for enhanced light harvesting. ACS Appl Mater Interfaces 3(3):721–725
21. Feng T, Xie D, Lin Y, Zang Y, Ren T, Song R, Zhao H, Tian H, Li X, Zhu H, Liu L (2011) Graphene based Schottky junction solar cells on patterned silicon-pillar-array substrate. Appl Phys Lett 99:233505–233501
22. Dong HS, Ju HK, Kim JH, Chan WJ, Sang WS, Lee HS, Kim S, Choi SH (2017) Graphene/porous silicon Schottky-junction solar cells. J Alloy Compd 715:291–296
23. Sarro PM, Brida D, Vlist W, Brida S (2000) Effect of surfactant on surface quality of silicon microstructures etched in saturated TMAHW solutions. Sensors Actuators A Physical 85(1–3):340–345
24. Swarnalatha V, Rao AN, Ashok A, Singh S, Pal P (2017) Modified TMAH based etchant for improved etching characteristics on Si{100} wafer. Journal of Micromechanics & Microengineering, 2017, 27(8):085003
25. Sun Z, Raji A, Zhu Y, Xiang C, Yan Z, Kittrell C, Samuel E, L G,Tour JM (2012) Large-Area Bernal-Stacked Bi^{-}, Tr^{-}, and Tetralayer Graphene. ACS Nano 6(11):9790–9796
26. Qi JL, Zheng WT, Zheng XH, Wang X, Tian HW (2011) Relatively low temperature synthesis of graphene by radio frequency plasma enhanced chemical vapor deposition. Appl Surf Sci 257(15):6531–6534
27. Terasawa T, Saiki K (2012) Growth of graphene on Cu by plasma enhanced chemical. vapor depositionCarbon 50(3):869–874
28. Ou WY, Zhang Y, Li H, Zhao L, Zhou C, Diao H, Liu M, Lu W, Zhang J, Wang W (2010) Texturization of mono-crystalline silicon solar cells in TMAH without the addition of surfactant. J Semicond 31(10):106002
29. Wang S, Weil BD, Li Y, Wang KX, Garnett E, Fan S, Cui Y (2013) Large-area free-standing ultrathin single-crystal silicon as processable materials. Nano Lett 13(9):4393–4398
30. Biswas K, Kal S (2006) Etch characteristics of KOH, TMAH and dual doped TMAH for bulk micromachining of silicon. Microelectronics journal 37(6):519–525
31. Chen PH, Peng HY, Hsieh CM, Chyu MK (2001) The characteristic behavior of TMAH water solution for anisotropic etching on both Silicon substrate and SiO_2 layer. Sensors Actuators A Physical 93(2):132–137
32. Fan Y, Han P, Peng L, Xing Y, Ye Z, Hu S (2013) Differences in etching characteristics of TMAH and KOH on preparing inverted pyramids for silicon solar cells. Appl Surf Sci 264:761–766
33. Zubel I, Rola K, Kramkowska M (2011) The effect of isopropyl alcohol concentration on the etching process of Si-substrates in KOH solutions. Sensors Actuators A Physical 171(2):436–445

34. Zubel I, Kramkowska M (2001) The effect of isopropyl alcohol on etching rate and roughness of (100) Si surface etched in KOH and TMAH solutions. Sensors Actuators: A Physical 93(2):138–147
35. Bartolomeo AD, Giubileo F, Luongo G, Iemmo L, Martucciello N, Niu G, Fraschke M, Skibitzki O, Schroeder T, Lupina G (2016) Tunable Schottky barrier and high responsivity in graphene/Si-nanotip optoelectronic device. 2D Materials 4(1):015024
36. Abdullah MF, Hashim AM (2019) Improved coverage of rGO film on Si inverted pyramidal microstructures for enhancing the photovoltaic of rGO/Si heterojunction solar cell. Mater Sci Semicond Process 96:137–144
37. Xie C, Zhang X, Wu Y, Zhang X, Zhang X, Wang Y, Zhang W, Gao P, Han Y, Jie J (2013) Surface passivation and band engineering: a way toward high efficiency graphene–planar Si solar cells. Journal of Materials Chemistry A 1(30):8567
38. Jiao K, Wang X, Yu W, Chen Y (2014) Graphene oxide as an effective interfacial layer for enhanced graphene/silicon solar cell performance. Journal of Materials Chemistry C 2:7715–7721
39. Abdullah MF, Hashim AM (2019) Review and assessment of photovoltaic performance of graphene/Si heterojunction solar cells. Journal of Materials Science 54:911–948
40. Liu H, Liu Y, Zhu D (2011) Chemical doping of graphene. J Mater Chem 21(10):3335–3345

Tables

Due to technical limitations, tables are only available as a download in the Supplemental Files section.

Figures

Fig. 1

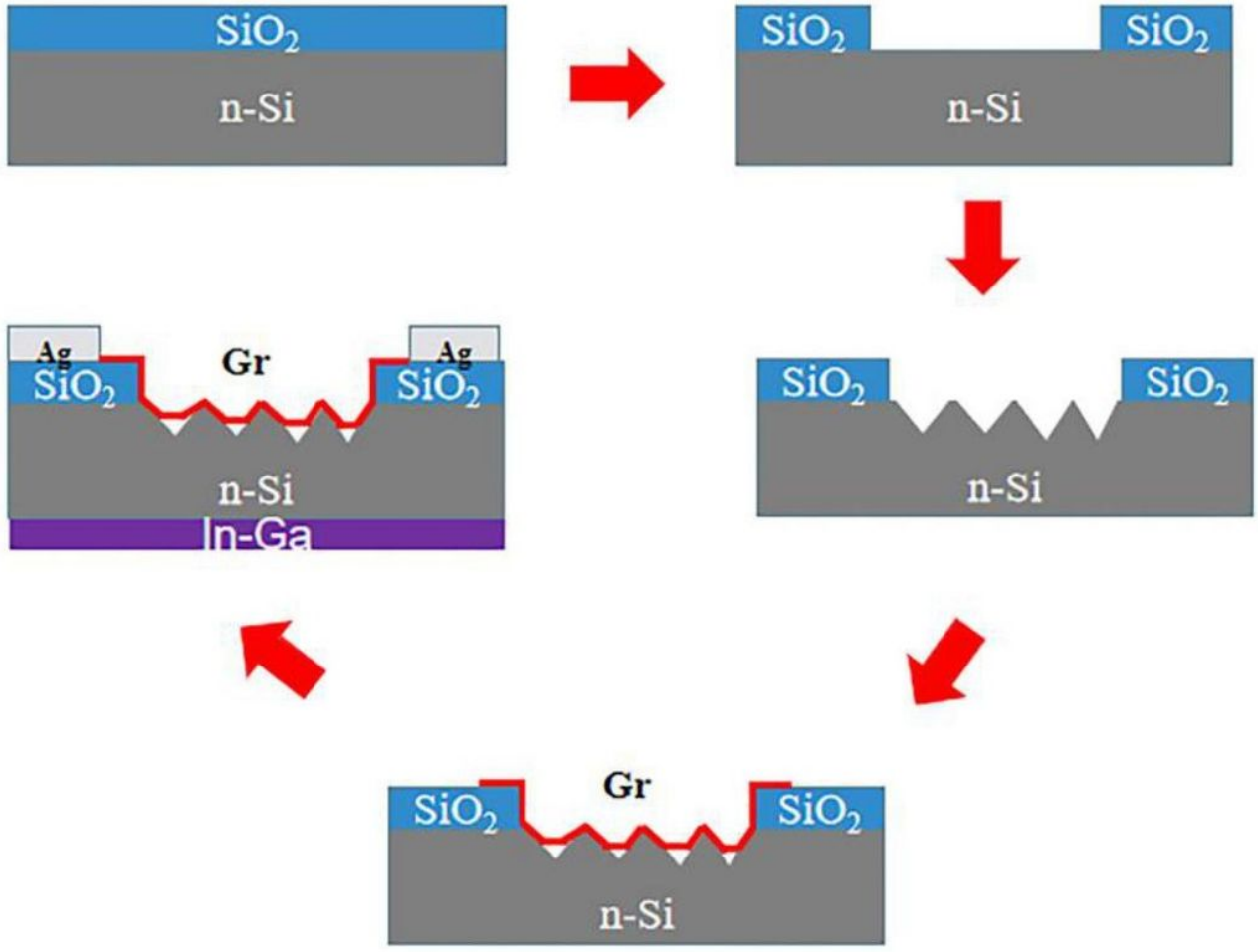

Figure 1

Schematic illustration for fabrication of Gr/SiPa Schottky junction solar cell.

Fig. 2

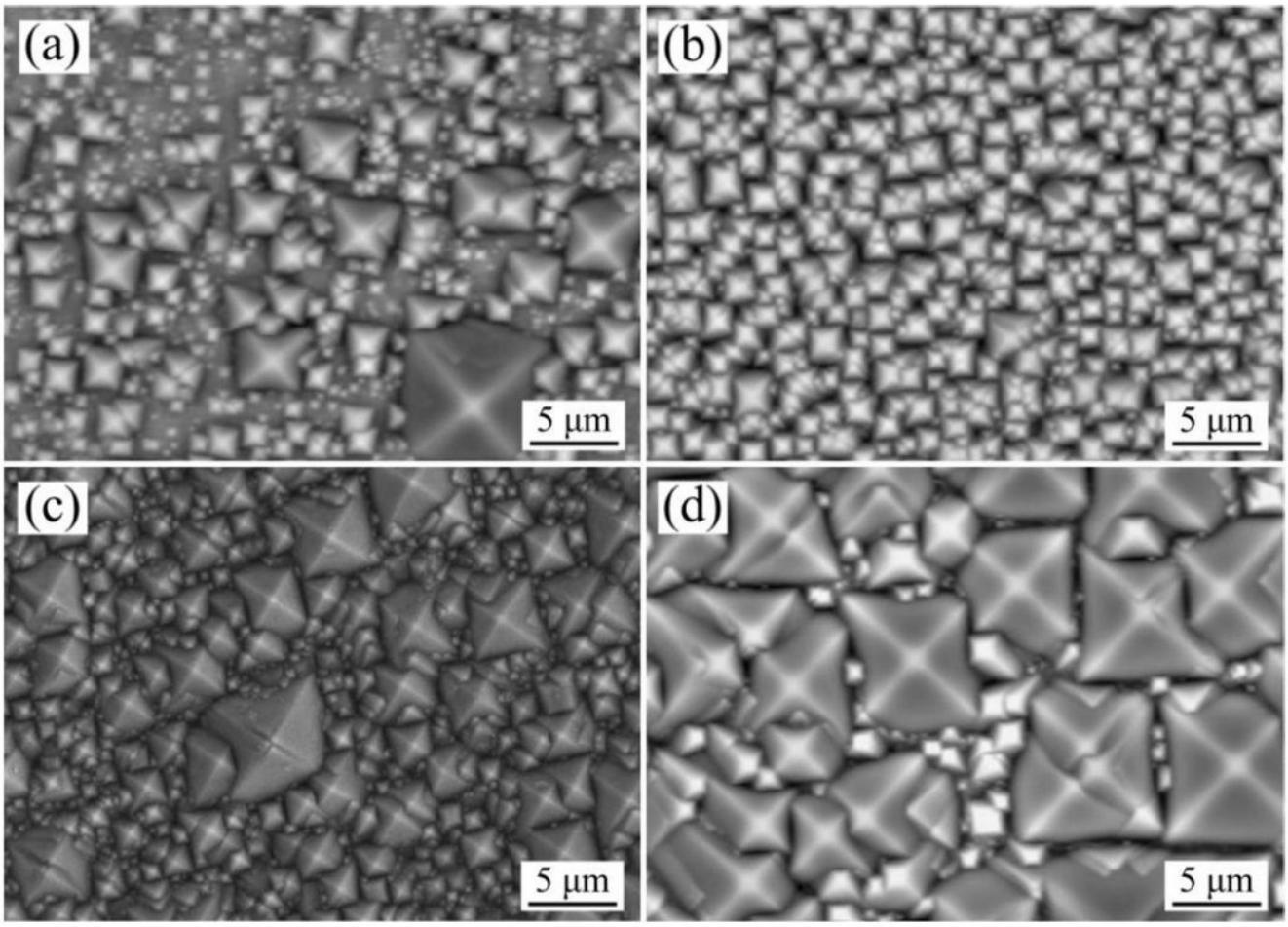

Figure 2

SEM images of SiPa with different TMAH concentration (a) 1%, (b) 2%, (c) 3%, (d) 4%.

Fig. 3

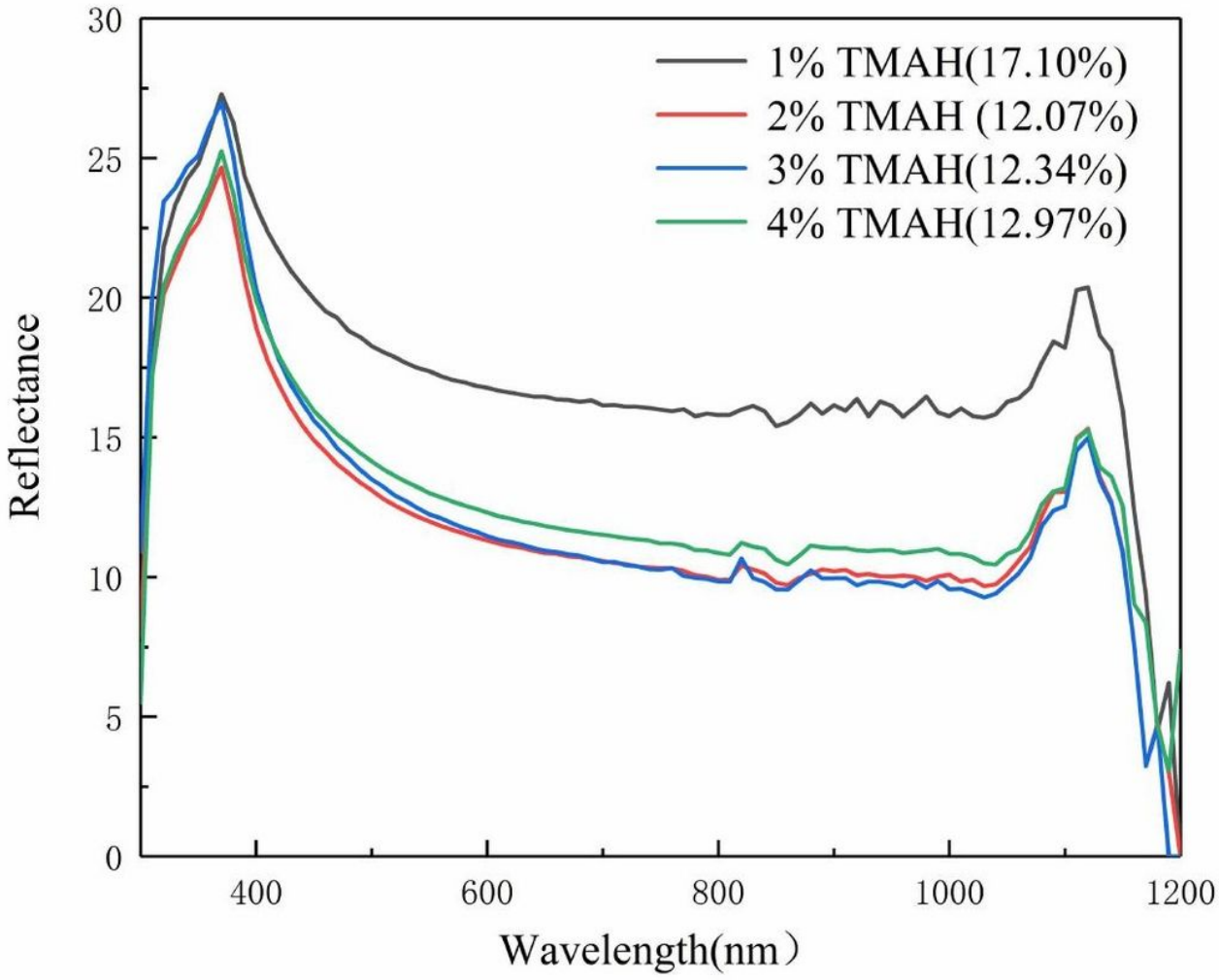

Figure 3

Reflection spectra of SiPa at different TMAH concentrations

Fig. 4

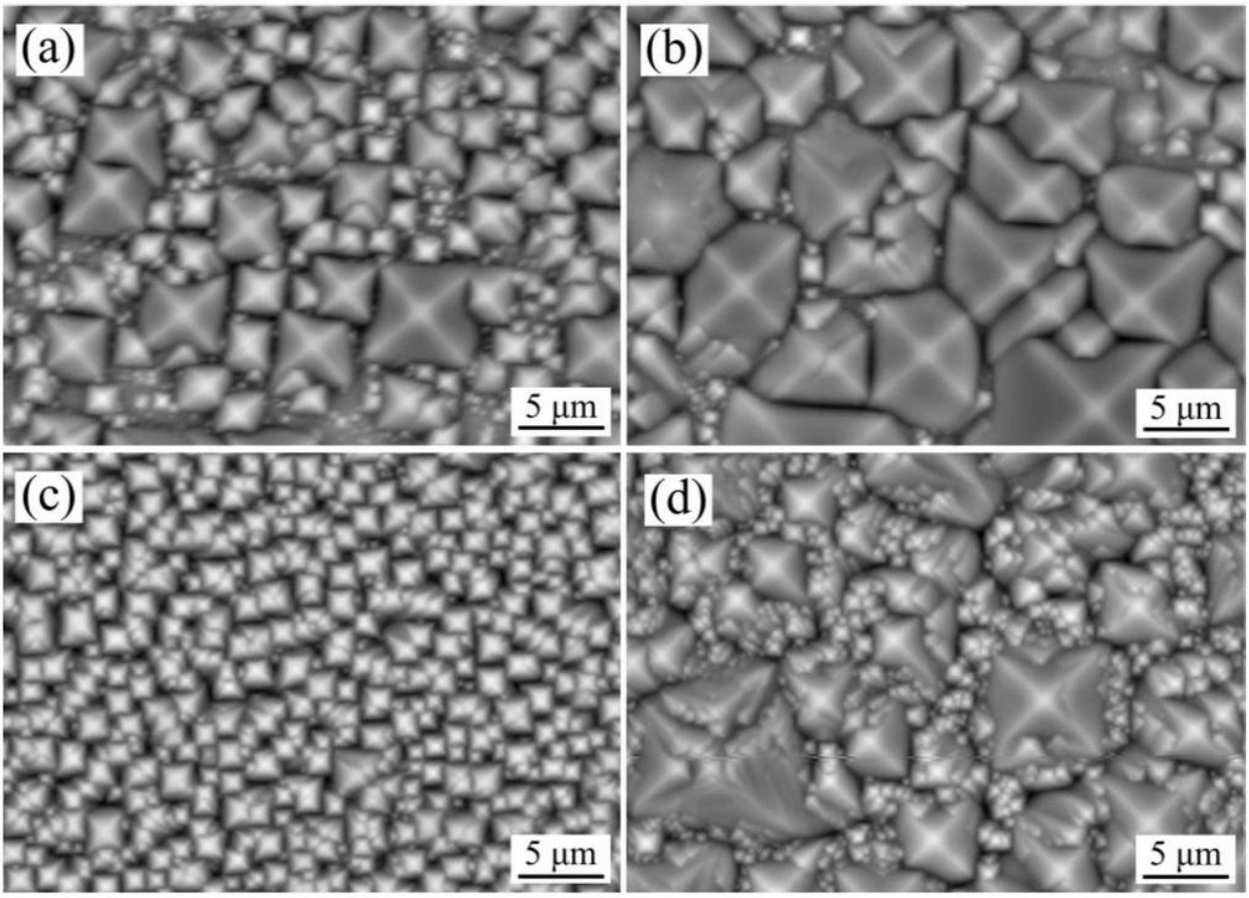

Figure 4

SEM images of SiPa with different IPA concentration (a) 0%, (b) 5%, (c) 10%, (d) 15%.

Fig. 5

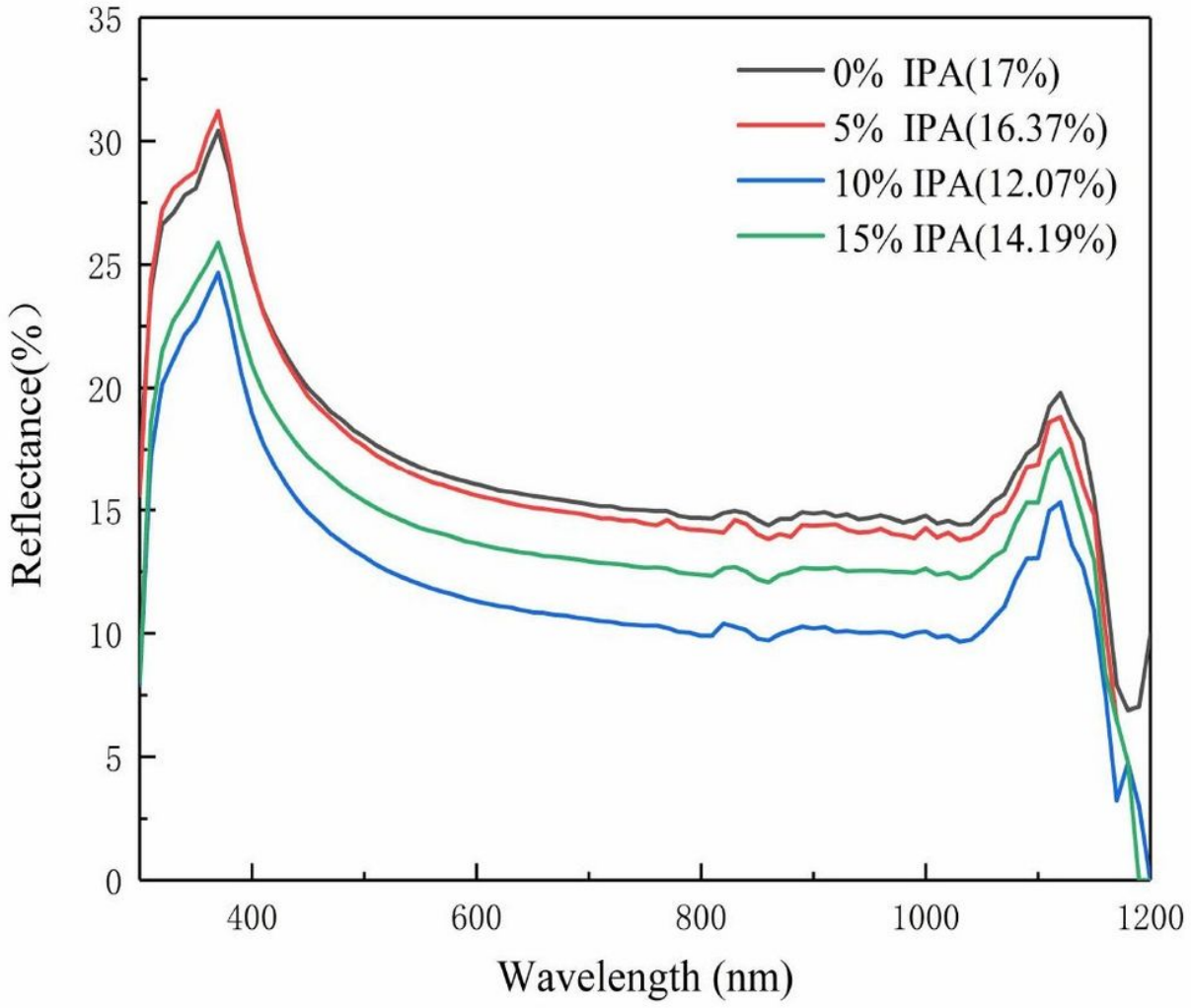

Figure 5

Reflection spectra of SiPa at different IPA concentrations

Fig. 6

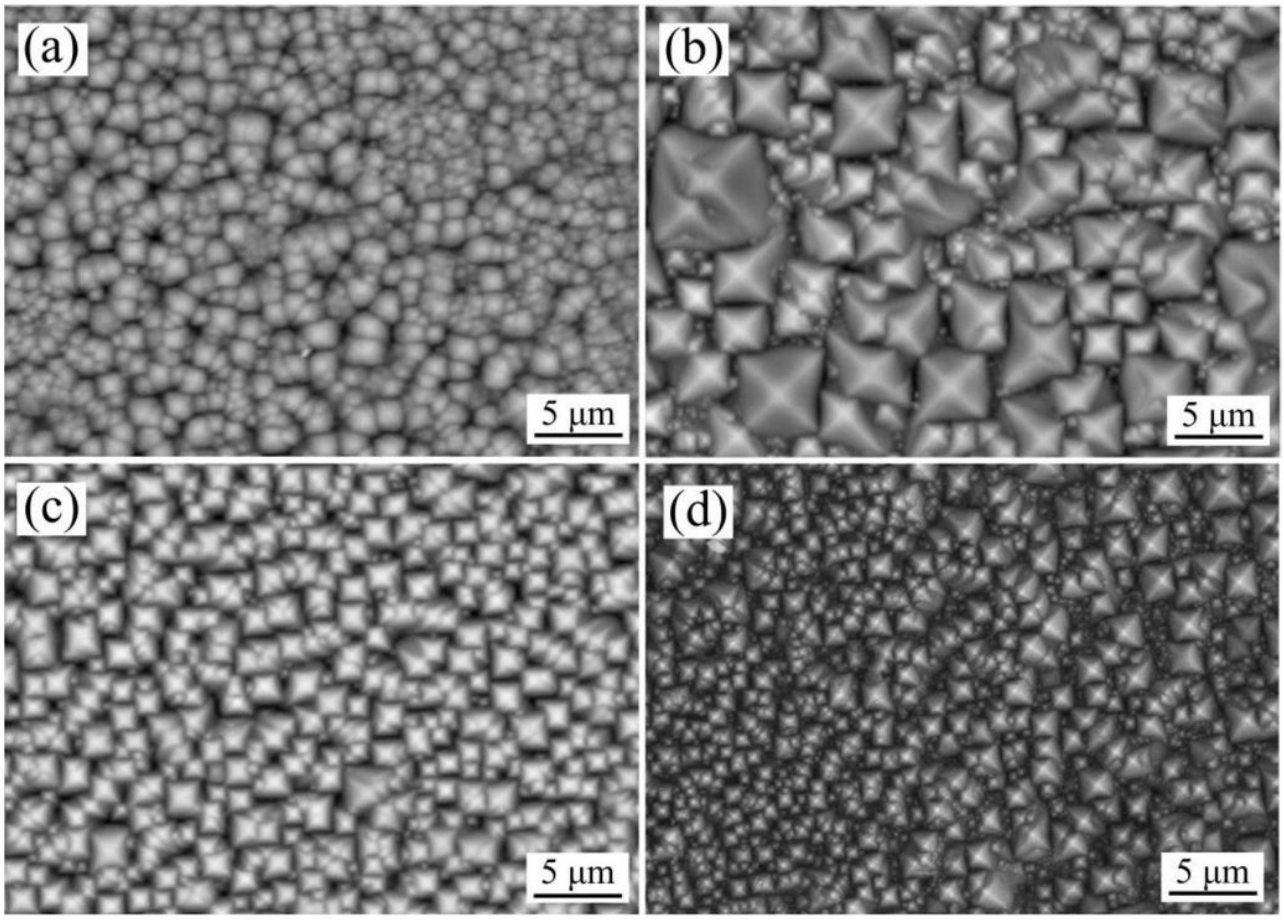

Figure 6

SEM images of SiPa with different etching time (a) 10 min,(b) 20 min,(c) 30 min,(d) 40 min.

Fig. 7

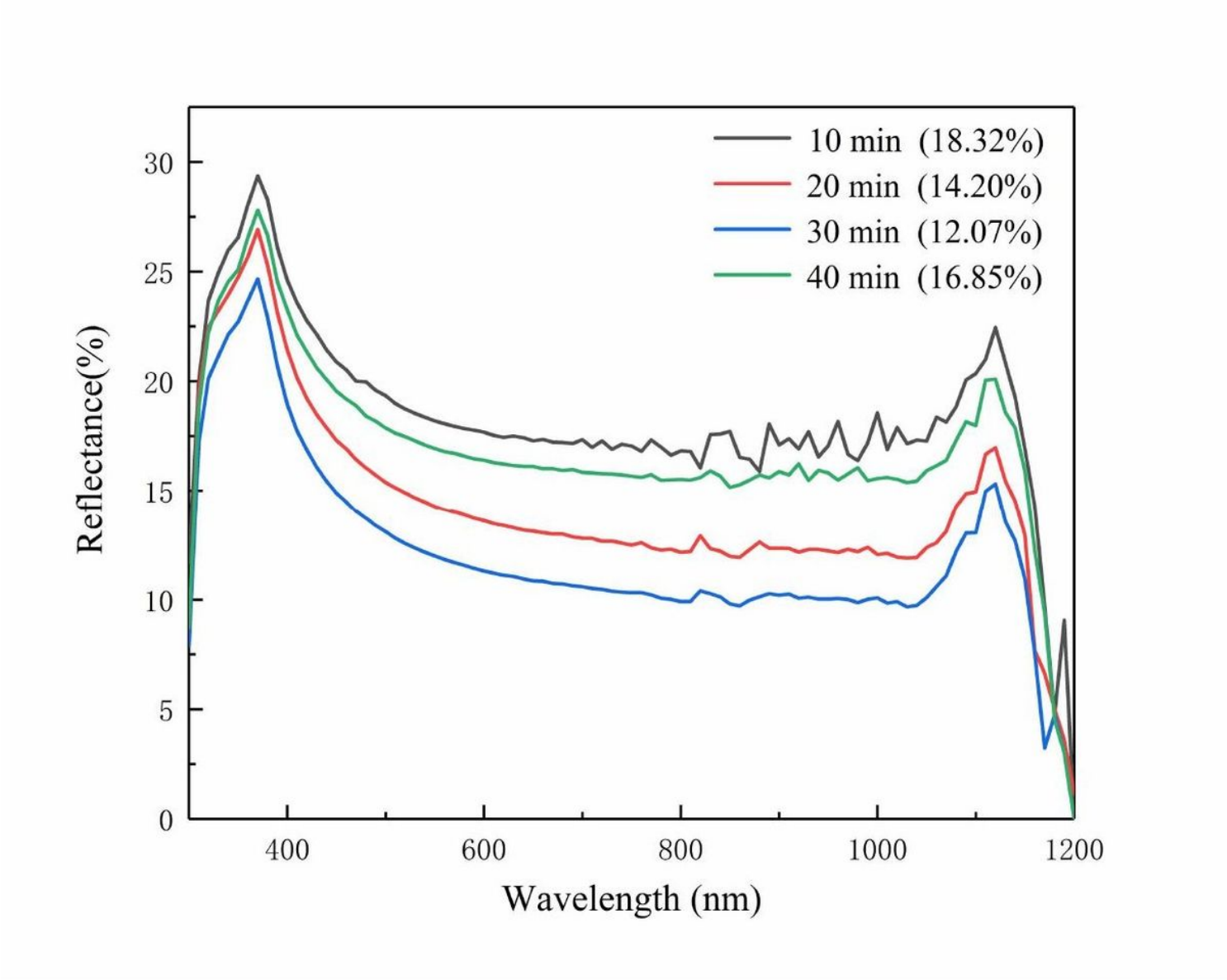

Figure 7

Reflection spectra of SiPa at different etching time

Fig. 8

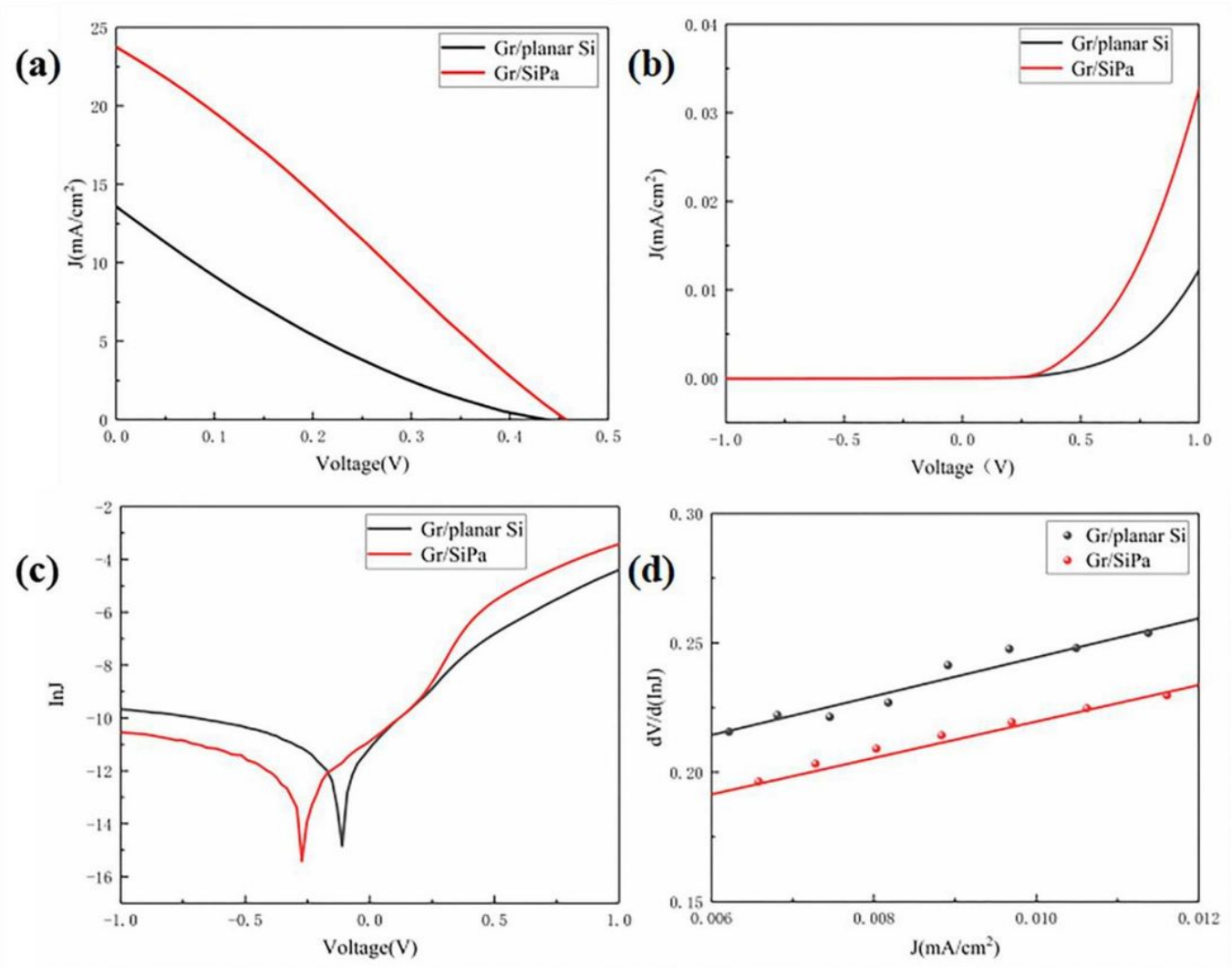

Figure 8

(a) Illuminates J-V characteristics curves. (b) Dark J-V characteristics curves. (c) Dark lnJ-V curves. (d) Plots of dV/d(lnJ)-J curves for Gr/planar Si solar cells and Gr/SiPa solar cells

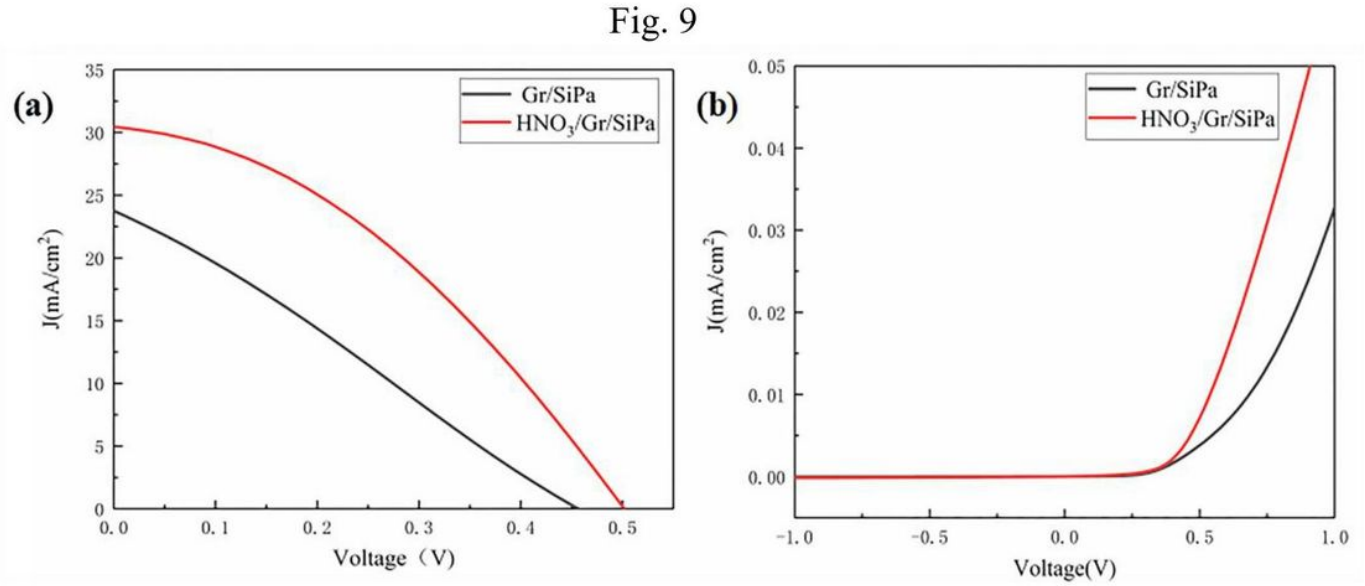

Figure 9

Illuminates(a) and dark (b) J-V characteristics curves for Gr/SiPa solar cells before and after HNO3 doping

Supplementary Files

This is a list of supplementary files associated with this preprint. Click to download.

- Tables.doc.pdf